

# Lawrence Berkeley National Laboratory

## Recent Work

### Title

TRANSVERSE-FIELD FOCUSING BEAM TRANSPORT EXPERIMENT

### Permalink

<https://escholarship.org/uc/item/6x592479>

### Author

Kwan, J.W.

### Publication Date

1986-10-01

2



# Lawrence Berkeley Laboratory

UNIVERSITY OF CALIFORNIA

## Accelerator & Fusion Research Division

RECEIVED  
LIBRARY  
SERIALS SECTION

JUL 9 1987

LIBRARY  
SERIALS SECTION

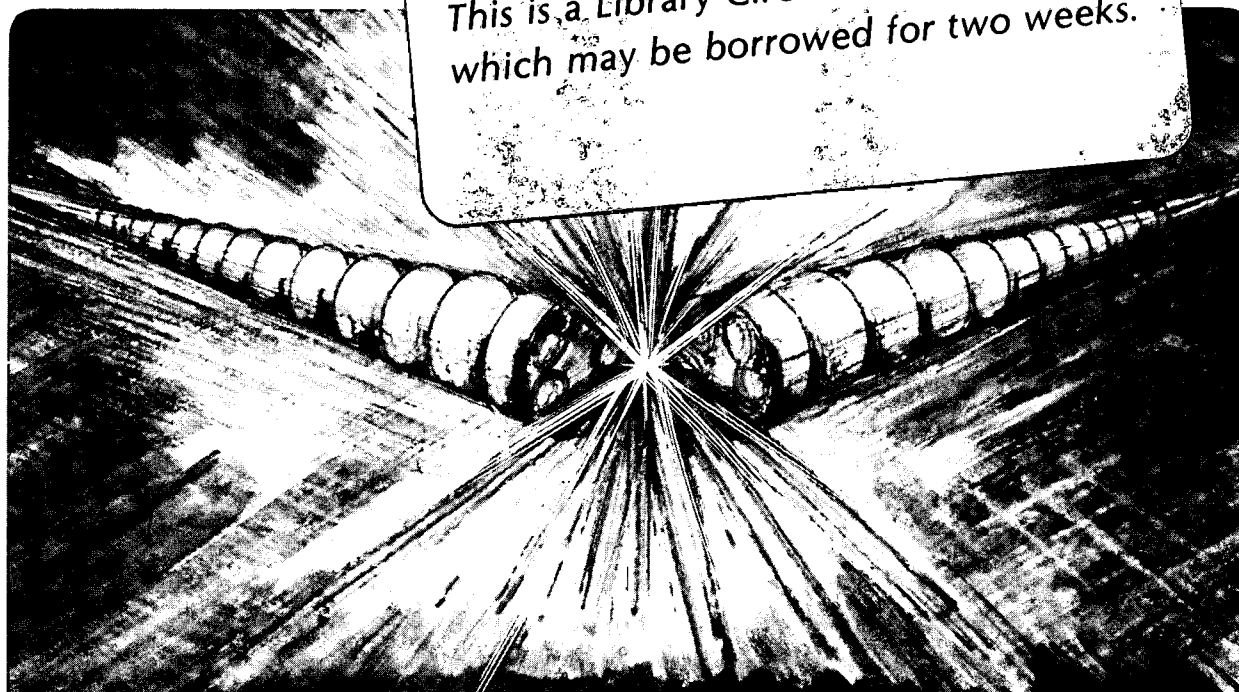
Presented at the Fourth International Symposium  
on the Production and Neutralization of Negative  
Ions and Beams, Upton, L.I., NY, October 27-31, 1986

### TRANSVERSE-FIELD FOCUSSED BEAM TRANSPORT EXPERIMENT

J.W. Kwan, G.D. Ackerman, O.A. Anderson, C.F. Chan,  
W.S. Cooper, L. Soroka, and W.F. Steele

October 1986

**TWO-WEEK LOAN COPY**  
This is a Library Circulating Copy  
which may be borrowed for two weeks.



LBL-22387  
2

## DISCLAIMER

This document was prepared as an account of work sponsored by the United States Government. While this document is believed to contain correct information, neither the United States Government nor any agency thereof, nor the Regents of the University of California, nor any of their employees, makes any warranty, express or implied, or assumes any legal responsibility for the accuracy, completeness, or usefulness of any information, apparatus, product, or process disclosed, or represents that its use would not infringe privately owned rights. Reference herein to any specific commercial product, process, or service by its trade name, trademark, manufacturer, or otherwise, does not necessarily constitute or imply its endorsement, recommendation, or favoring by the United States Government or any agency thereof, or the Regents of the University of California. The views and opinions of authors expressed herein do not necessarily state or reflect those of the United States Government or any agency thereof or the Regents of the University of California.

## TRANSVERSE-FIELD FOCUSSED BEAM TRANSPORT EXPERIMENT

J. W. Kwan, G. D. Ackerman, O. A. Anderson, C. F. Chan,  
W. S. Cooper, L. Soroka, and W. F. Steele

Lawrence Berkeley Laboratory  
University of California  
Berkeley, CA 94720

### ABSTRACT

The Transverse-Field Focussing (TFF) beam transport and accelerator system developed at LBL is useful for negative-ion-based neutral beam injection due to its unique differential pumping and neutron shielding properties. We have tested the first module of our TFF system transporting  $H^-$  beams up to 80 keV beam energy. The testing addressed the most crucial physics and engineering issues involved in the principles of a TFF system including beam compression and differential gas pumping. At optimum perveance, the present design will transport 4 A/m of  $H^-$  beam at 80 keV beam energy.

### INTRODUCTION

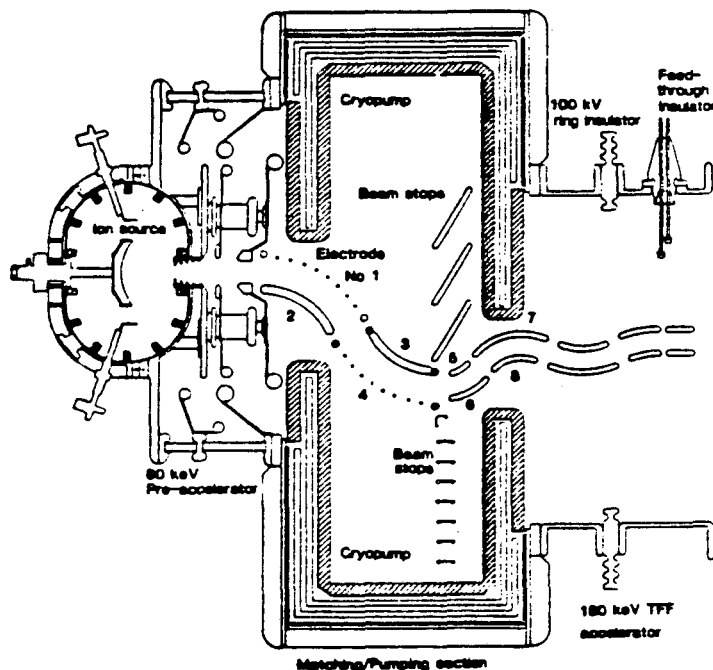
In a conventional neutral beam injection system, the neutrons produced by the reacting plasma in a fusion reactor can travel back into the neutral beam system causing radiation damage and contamination to the beamline components. The Transverse Field Focussing (TFF) beam transport and accelerator system developed at LBL can solve this problem by transporting the ion beam through several bends in a neutron shielding region before converting the beam to neutrals, thus protecting the ion source and the accelerator from the energetic neutrons.<sup>1</sup> An additional advantage in the TFF beam transport system is that differential gas pumping can be applied to quickly pump away the hydrogen gas in the beamline. This unique differential pumping characteristic is important in reducing the loss by premature electron detachment of a  $H^-$  beam by the background hydrogen gas.<sup>2</sup> Substantial beam losses can significantly affect the overall performance of a neutral beam injector.

The TFF system makes use of the focussing ability of the transverse field between a pair of concentric cylindrical electrode plates.<sup>3</sup> Charged particles with the correct initial velocity will be able to travel along the channel in between the electrodes in such a way that the electrostatic force is balanced by the centrifugal force. Hence the TFF system is inherently a 2-dimensional system which transports ribbon-shaped beams. The third dimension (in the y-axis) is usually limited by the length of the negative ion source being used. The transverse field can also compress the beam width. Typically the beam width is about 1.5 cm which corresponds to a current density of 27 mA/cm<sup>2</sup>.

The original design of our TFF system is supposed to transport more than 4A of  $H^-$  per meter of source length.<sup>4</sup>

### EXPERIMENTAL SET-UP

Figure 1 shows a plan view of the experimental set-up. The negative hydrogen ion beam, produced by a surface-conversion  $H^-$  source, is accelerated by a conventional single-slot accelerator (called the pre-accelerator) to an initial energy as required by the TFF system. Details of the design and testing of the ion source and the pre-accelerator have been reported elsewhere.<sup>5</sup> The ion source together with the pre-accelerator have been tested to produce 1 A of 80 keV  $H^-$  beam for 30 sec (the ion source is



LBL 8510-4457

Fig. 1. Plan view of the TFF beam transport experimental set-up.

capable of producing more than 1.25 A of  $H^-$ ). Typical beam data taken at the exit of the pre-accelerator in absence of the TFF beam transport section are summarized in Table 1.

Both the surface-conversion  $H^-$  source and the pre-accelerator have problems related to beam uniformity along the slot length. The first problem is that it is difficult to maintain a spatially uniform  $H^-$  production in a large surface-conversion source when neither the cesium coverage on the converter surface nor the plasma density in front of the converter are very uniform.<sup>6</sup> The variation in  $H^-$  intensity can be greater than 20%. This effect is more pronounced at the edge than in the

middle part of the converter.

The second problem lies in focussing of the ion beam by the ends of the aperture slot in the pre-accelerator. This end-of-slot effect is basically a three dimensional beam aberration problem which happens where the two dimensional planar symmetry fails to hold at the slot ends. The ions near the ends of the slot are deflected toward the center thus producing a nonuniform current density profile. The effect can be minimized, but not completely eliminated, by reducing the Pierce angle on the ends of the beam-forming electrode. Fig. 2 compares the typical H<sup>-</sup> current density profiles along the slot length (after integrating the beam intensity across the short direction) before and after making the end corrections. This problem becomes less important as the slot length becomes much longer than the slot width.

Table 1. Typical beam data taken at the exit of the pre-accelerator in absence of the TFF beam transport system.

---

Beam current	up to 1 A (25 cm slot length)
Beam energy	up to 80 keV
Optimum perveance	$4.4 \times 10^{-8} \text{ A/V}^{3/2}$
Uniformity along slot	$\pm 20\%$
Electron fraction	12%
Pulse length	30 sec
Normalized x-emittance	0.45 $\mu$ mrad-cm (90% contour)
Beam temperature	11.2 eV

---

Immediately following the pre-accelerator is the first section of the TFF beam transport system. This section is called the matching and pumping (M/P) section because besides transporting the ion beam it also serves the dual purposes of compressing the beam width to match the requirement of any subsequent TFF accelerator and pumping away the gas from the source rapidly.<sup>2</sup> It consists of two sets of curved electrodes (electrode number 1 through 4 in Fig. 1), which will transport the beam through two linked 70 degree bends. The electrodes with the larger radius are made up of parallel tubes so that there are large openings for vacuum pumping. The smaller radius electrodes are solid plates which act as partitions to separate the TFF chamber into two halves thus providing an effective differential pumping arrangement. All the electrodes are water-cooled. Vacuum pumping is done by ultra-thin cryopanel (developed at LBL) placed along the sidewall of the chamber.<sup>7</sup> The cryopanel are protected from any neutralized H<sup>-</sup> beam particles by the beam stops as shown in Fig. 1. Also shown in the figure are the electrodes for the 180-keV TFF accelerator. This part of the TFF system will not be tested due to budget limitations despite the fact that many parts of the accelerator are already built. In testing the TFF M/P section without the 180-keV TFF accelerator, electrodes number 5 and 6 are replaced with a pair of flat plates

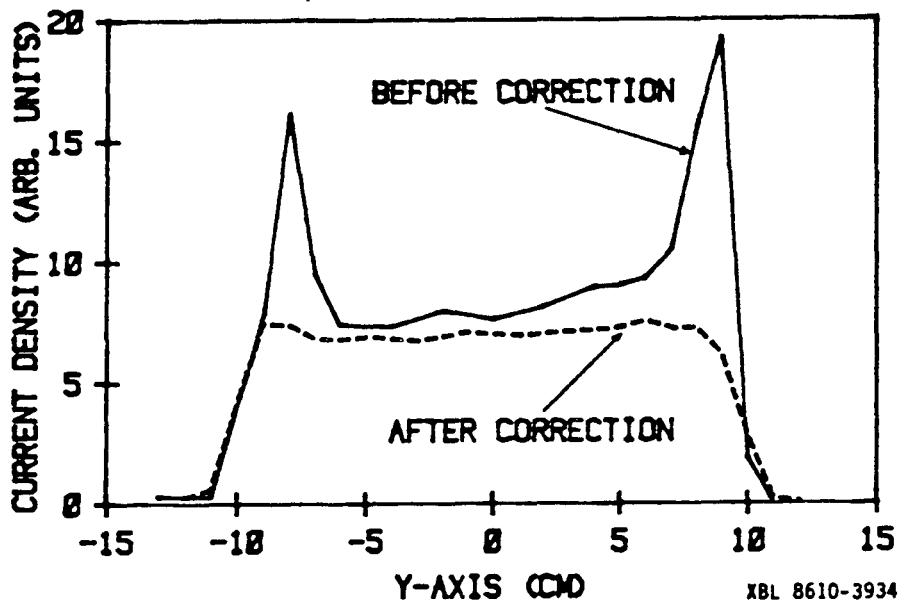


Fig. 2. Typical  $H^-$  current density profiles along the slot length before and after the end corrections.

used as steering electrodes.

Like all other negative ion sources, the surface-conversion source produces electrons as well as  $H^-$  ions. The electrons are accelerated together with the  $H^-$  ions through the pre-accelerator. At the exit of the pre-accelerator we find that the electron fraction in the beam is about 10%. This is an upper limit of the amount of electrons leaving the ion source because included in the 10% are electrons being generated inside the pre-accelerator due to electron detachment from the  $H^-$  ions and also secondary electrons emitted from the gradient electrode but not collected by the suppressor. Ideally, none of the electrons can get through the TFF M/P section. Any electron in the beam will be removed from the ions by a transverse magnetic field at the second bend of the TFF M/P section; the electrons will be collected on electrode number 3.

The ion beam leaving the TFF will be diagnosed by two emittance scanners and a pair of small-aperture (1.5 mm diameter) mass analysers which are capable of distinguishing heavy ions from electrons.<sup>5</sup> Both the emittance scanners and the mass analysers are located at 40.6 cm downstream of the TFF M/P section exit. Results of the x-emittance measurement can be compared with predictions from our beam optics code (WOLF). The y-emittance will provide useful information on the temperature of the  $H^-$  ions coming from a Cesium surface-conversion source. The mass analysers measure the ion beam intensity and the electron fraction which in turn gives an estimation of the total beam loss during acceleration and transport.

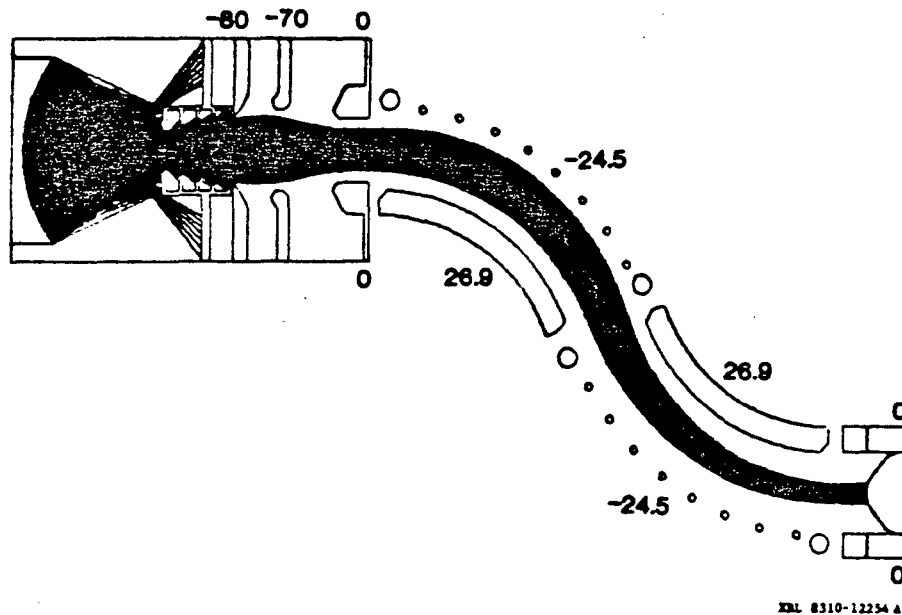


Fig. 3. Ion trajectories obtained from WOLF code calculation, the voltage bias on the electrodes are indicated in the figure.

#### TEST RESULTS

One 80-kV power supply is required to operate the pre-accelerator and two separate 30-kV power supplies to operate the TFF M/P section. The voltage on the gradient electrode is obtained from the 80-kV power supply using a resistive divider. All three power supplies are voltage regulated to within 0.3% of the operating voltages. A deviation of 1% in the accelerating voltage can amount to 14 mrad deflection in the final beam steering. Likewise, a 1% change in the TFF electrode voltage will produce a deflection of 8 mrad. The design values of the voltage on each electrode (according to WOLF code) are depicted in Fig. 3; these numbers are very close to the ones we have used in the experiment to properly steer the beam through the TFF. In running beams of energy lower than 80keV, one simply scales down the voltages on all the electrodes by the same factor and reduces the beam current according to the "three-halves" law in order to keep the perveance constant. Also shown in Fig. 3 are the ion trajectories computed with the space-charge effect taken into consideration.

We have operated the TFF M/P section with the pre-accelerator to transport  $H^-$  beam currents up to 640 mA and energies up to 80 keV. The beam pulse length was limited by breakdown in the TFF section. It appeared that some insulators failed to hold voltage after accumulating charged particles during a beam pulse. The pulse length is less at higher beam currents and energies. At 48 kV, we were able to transport 320 mA of  $H^-$  beam for over 430 msec, but at 80 kV the pulse length was only



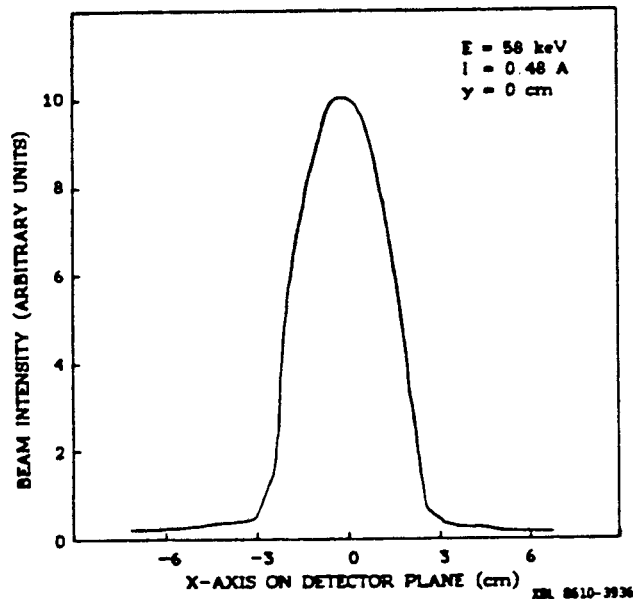


Fig. 4  $H^-$  ion beam intensity profile obtained at 40 cm downstream of the TFF exit.

40 msec long. Nevertheless 40 msec was long enough to perform beam diagnostics and to demonstrate that the beam was properly steered through the TFF transport system without running into the electrodes. No damage to the TFF electrodes or the supporting insulators could be found after the experiment. We think that the breakdown problem can be solved by adding shields to protect any exposed insulator surfaces, but the experiment had to be terminated before this problem could be solved.

Fig. 4 shows a typical intensity profile of the  $H^-$  ribbon beam in the short direction of the slot (the x-direction), near the vertical center ( $y=0$ ), measured with the mass analyser. The location of the peak is a quick reference of the amount of beam steering. The amount of electrons measured in the beam is so small that it can be ignored. The mass analyser was scanned up to 6.5 cm on each side of the centerline in order to make sure that there is no satellite beam missed by the emittance scanner.

The TFF M/P section was designed with a carefully shaped contour at the top and bottom ends of the electrodes in order to produce electrostatic barriers to confine the beam to within 25 cm. Unfortunately the length of the beam was reduced from 25 cm to 20 cm when we added shields to the beam forming electrode in order to correct the end-of-slot focussing effect in the pre-accelerator. Hence, without changing the location of the electrostatic barriers, the beam coming out of the pre-accelerator can expand from 20 cm up to the 25 cm limit. At the beam edge, the  $H^-$  ion velocity will become diverging as a result of the space charge expansion. The TFF beam edge confinement scheme has therefore never been fully tested although

we have not detected any beam beyond the 25 cm limit (see the y-emittance diagram in Fig. 7).

The current density nonuniformity has a significant impact on the beam optics because it is impossible to maintain optimum perveance throughout the entire slot length. A condition where the center of the beam is at optimum perveance would imply that the beam edge is always "underdense". Thus the correct numerical value of the optimum perveance in this condition is equal to  $I_c / (V_{acc})^{3/2}$  where  $I_c$  is the product of 20 cm times the current density at the center and  $V_{acc}$  is the final beam energy. Experimentally, we found the optimum perveance to be about  $3.6 \times 10^{-8} \text{ A/V}^{3/2}$ , which corresponds to 4 A/m of  $H^-$  beam at 80 keV beam energy as expected.

The total detectable beam current ( $I_t$ ), obtained by integrating the mass analyser signal in both x and y directions, can be compared with the electrical current ( $I_d$ ) entering the ion source from the 80-kV power supply. The total beam loss fraction is given as

$$f = 1 - I_t / (I_d - I_e)$$

where  $I_e$  is the electron current leaving the ion source which is approximately equal to 10% of  $I_d$  or less. Naturally, the amount of beam loss depends significantly on the beamline pressure. At 1 mTorr of gas pressure in the source (gas flow = 130 SCCM) and with cryopumping,  $f$  is about equal to 15%. Without cryopumping,  $f$  is in the order of 33%. It is obvious why we want a pumping section in the beamline before the beam can be accelerated to higher energy.

It is interesting to observe the electrical currents drawn to the TFF electrodes. Fig. 5 shows the variation of these currents with gas flow for a 42 keV beam without cryopumping. The linear dependence of the electrode currents agrees with the model that the origin of these currents is secondary electron emission resulting from the impact of neutrals (created by electron detachment of the  $H^-$  ions) on the negative TFF electrodes. Any direct beam interception by the electrodes would produce an intercept on the graph in Fig. 5 indicating a finite amount of electrode currents at zero gas flow. This is completely in agreement with our experience in beam steering. A well steered beam would produce an intercept near the origin like the one shown in Fig. 5, and a badly steered beam would have an intercept far away from the origin.

Projectional emittance of the ion beam at the exit of the TFF section was measured with two double-slit emittance scanners, one in each plane. The entrance slit of the scanner is 3 cm long and 0.01 cm wide. The resultant emittance diagrams are shown in Fig. 6 and Fig. 7. First, we will discuss the x-emittance. According to the emittance diagram, there is no sign of significant beam aberration introduced by the TFF transport system. The normalized emittance value, associated with the area included in

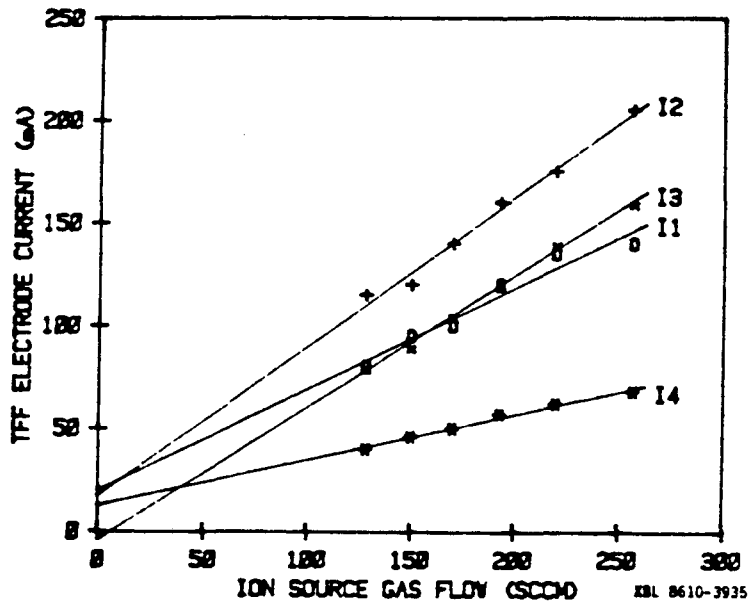


Fig. 5 TFF electrode currents as a function of ion source gas flow

the 90% beam fraction contour, for the beam transported through the TFF M/P section agreed with the value that we found earlier when we were operating the pre-accelerator alone to within 15%. Thus there is little emittance growth occurred in the TFF beam transport section.

The emittance diagram also shows that the width of the beam at the exit plane of the TFF system is about 1.5 cm provided that we ignore the "wings" of the beam which contribute to only a small percentage of the total beam current. This beam width is in excellent agreement with the prediction from WOLF code simulation (see Fig. 3). The -0.4 cm offset of beam center in the emittance diagram is considered to be an alignment error.

Now we will examine the y-emittance data. Since the system is basically a slot geometry, we would expect the y-emittance to look like a stack of rectangles. This is more or less what happens at the center portion of the slot. However the beam edges are diverging due to the end-of-slot effect discussed earlier.

Since there is no focussing effect in the y-direction (except at the very ends), the angular distribution of the  $H^-$  ion intensity measured by the emittance scanner near  $y = 0$  cm is the actual angular distribution when the ions leave the converter. A typical profile of the angular distribution of a 40-keV beam is shown in Fig. 8. The half width of the distribution at the 1/e intensity level is 16.75 mrad. This corresponds to a transverse energy of 11.2 eV. This ion temperature is almost as high as the one obtained by A. Lietzke<sup>6</sup> using a different method of measurement. It is also interesting to note the maximum transverse energy. The profile shows that  $H^-$  ions were detected up to an

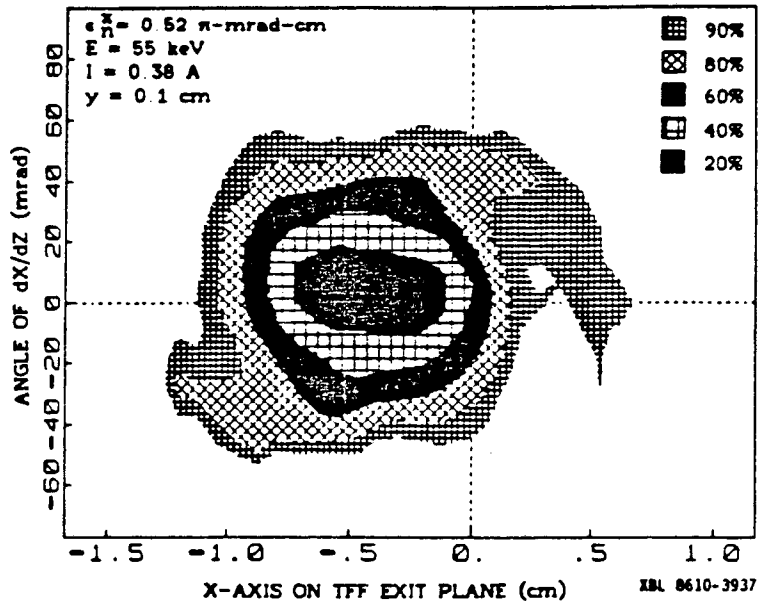


Fig. 6. x-emittance diagram

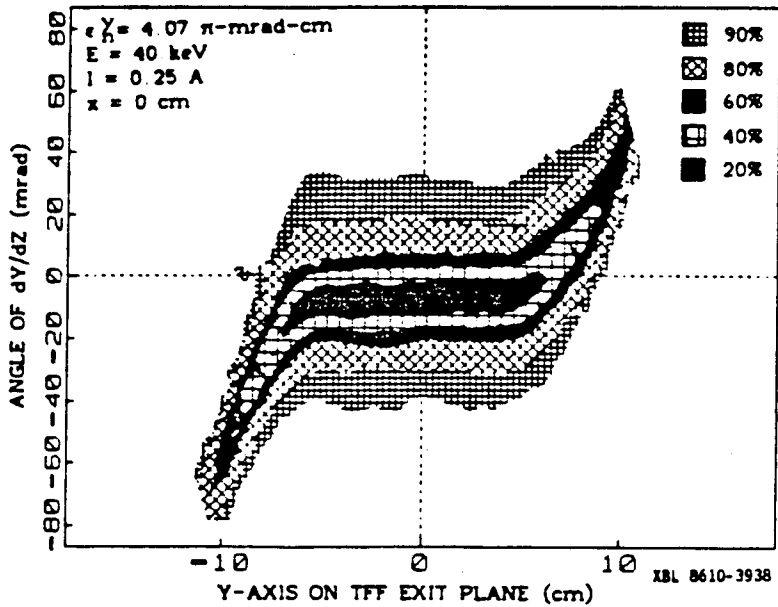


Fig. 7. y-emittance diagram

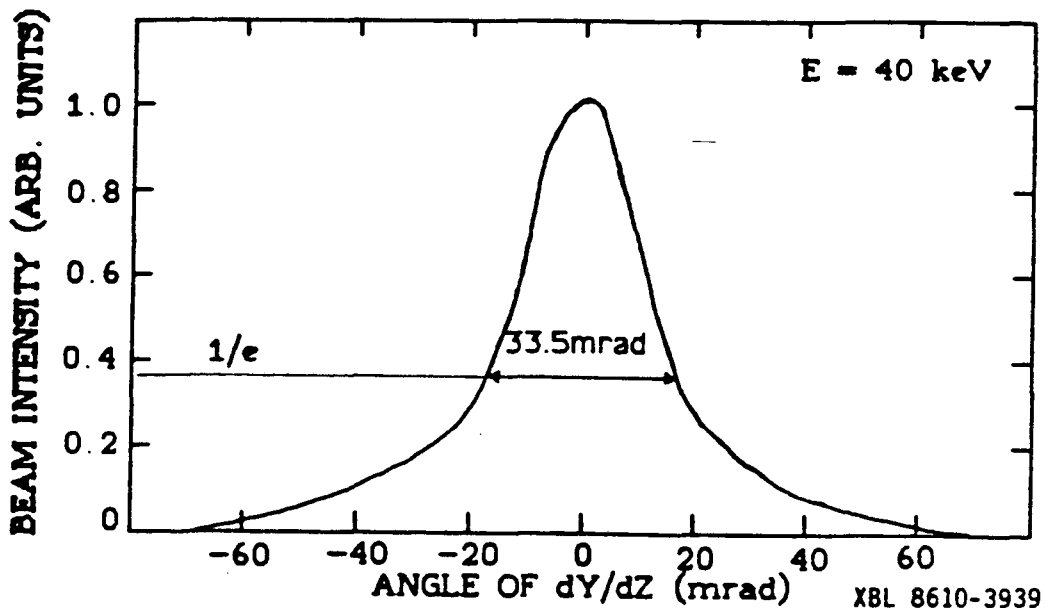


Fig. 8. Angular distribution of  $H^-$  intensity in the unfocused direction

angle of 70 mrad which corresponds to a transverse energy of 196 eV. Since the converter voltage was approximately -100 V with respect to the plasma, the maximum transverse energy was therefore approximately twice the converter voltage.

#### CONCLUSION

We have transported 640 mA of  $H^-$  ion beam at 80 keV energy through the TFF M/P section. The experimental results agreed very well with the design parameters. The cryopumping was very effective; it reduced the total beam loss to less than 15%.

The beam pulse length is limited by voltage breakdown in the TFF—at 80 keV it is 40 msec, but at 40 keV it can be as long as 0.5 sec. The beam edge confinement scheme in the TFF section has not been fully tested yet due to an indirect result of the end-of-slot beam focussing problem in the pre-accelerator. These two problems could be solved if we were given more time to continue the development; they are not problems associated with the fundamental physics issues of TFF beam transport system. The TFF system remains attractive for neutral beam injection in view of its pumping and neutron shielding properties, and its demonstrated ability to transport a beam with little loss and with little emittance growth.

\* This work is supported by US DOE contract no. DE-AC03-76SF00098.

## REFERENCE

1. W. S. Cooper, Proc. of the 3rd International Symposium on the Production and Neutralization of Negative Ions and Beams (Brookhaven, New York), p605 (1983).
2. O. A. Anderson, C. F. Chan, W. S. Cooper, J. W. Kwan, C. A. Matuk, H. M. Owren, J. A. Paterson, P. Purgalis and L. Soroka, IEEE Trans. on Nuclear Sci., NS-32 (5), p3509, (1985).
3. O. A. Anderson, Proc. of the 3rd International Symposium on the Production and Neutralization of Negative Ions and Beams (Brookhaven, New York), p473 (1983).
4. W. S. Cooper, O. A. Anderson, J. W. Kwan, and W. F. Steele, Proc. 11th Symposium on Fusion Engineering, Austin, Texas, p110, (1985).
5. J. W. Kwan, G. D. Ackerman, O. A. Anderson, C. F. Chan, W. S. Cooper, G. J. deVries, A. F. Lietzke, L. Soroka, and W. F. Steele, Rev. Sci. Instrum., 57 (5), p831, (1986).
6. A.F. Lietzke, K.W. Ehlers and K.N. Leung, Proc. of the 3rd International Symposium on the Production and Neutralization of Negative Ions and Beams (Brookhaven, New York), p344 (1983).
7. P. Purgalis, G. Ackerman, J. W. Kwan, J. A. Paterson, and A. H. Wandesforde, Proc. 11th Symposium on Fusion Engineering, Austin, Texas, p497, (1985).

This report was done with support from the Department of Energy. Any conclusions or opinions expressed in this report represent solely those of the author(s) and not necessarily those of The Regents of the University of California, the Lawrence Berkeley Laboratory or the Department of Energy.

Reference to a company or product name does not imply approval or recommendation of the product by the University of California or the U.S. Department of Energy to the exclusion of others that may be suitable.

*LAWRENCE BERKELEY LABORATORY  
TECHNICAL INFORMATION DEPARTMENT  
UNIVERSITY OF CALIFORNIA  
BERKELEY, CALIFORNIA 94720*